Computational Identification of Potential RET Inhibitors for Targeted Lung Cancer Therapy through Molecular Docking and ADMET Profiling

A. S., Sulaiman

aminusuleimanshehu8@gmail.com

Mewar University Gangrar

P. K., Teli
Mewar University Gangrar

R., Dhakar
Mewar University Gangrar

H. A., Muhammad
Bayero University

F., Chaturvedi
Mewar University Gangrar

I. M., Ibrahim
Mewar University Gangrar

Research Article

Additional Declarations: No competing interests reported.

Computational Identification of Potential RET Inhibitors for Targeted Lung Cancer Therapy through Molecular Docking and ADMET Profiling

Abstract

Lung cancer, a leading cause of cancer-related mortality, often involves aberrations in the RET (Rearranged during Transfection) gene, making it a critical target for therapeutic intervention. This study aims to identify potential small molecule inhibitors for the RET protein through molecular docking, to enhance treatment options for RET-associated lung cancer. The 3D structure of the RET protein was obtained from the PDB database, and a library of 901 ligand molecules was sourced from SelleckChem. Refinement of this library using FAF-Drugs4 resulted in 266 molecules suitable for further analysis based on drug-like properties and ADMET profiles. Molecular docking simulations revealed that seven out of ten ligands formed at least one hydrogen bond with the RET protein, with Pyracarbolid exhibiting the highest number. Fenuron heptanoate, Bis(phenylthioureido)carbamoyl-ethanediyl, Fluorolintane, and Sulfanilamide-4-chlorobenzoyl chloride showed moderate interactions, while Phthalimide and Thalidomide formed the fewest hydrogen bonds. This study's docking analysis identified potential lead compounds with favorable binding characteristics, contributing to our understanding of ligand-receptor interactions and offering insights into the design of new drugs targeting the RET protein receptor.

INTRODUCTION

The RET oncogene, short for "REarranged during Transfection," was discovered in 1985 when human lymphoma DNA was transfected into NIH3T3 cells, leading to the identification of a new transforming gene[1]. This transforming gene was created by the recombination of two unlinked human DNA sequences during transfection[2]. The RET proto-oncogene encodes a transmembrane receptor tyrosine kinase and its alterations can lead to various cancers and developmental disorders[1]. Gain-of-function mutations resulting from gene rearrangements have been observed in papillary thyroid carcinoma, non-small-cell lung carcinoma, and other cancers. On the other hand, point mutations are responsible for hereditary cancer syndrome, multiple endocrine neoplasia type 2, and sporadic medullary thyroid carcinoma[3]. The RET proto-oncogene codes for a receptor tyrosine kinase for members of the glial cell line-derived neurotrophic factor (GDNF) family of extracellular signaling molecules[4]. Loss-of-function mutations in RET are associated with Hirschsprung's disease, while gain-of-function mutations are associated with various types of human cancer[5]. The RET gene is located on chromosome 10 (10q11.2) and consists of 21 exons[6]. The natural alternative splicing of the RET gene results in the production of three different isoforms of the protein RET: RET51, RET43, and RET9, which contain 51, 43, and 9 amino acids in their C-terminal tail, respectively[2,4].

The Rearranged during Transfection (RET) gene is associated with certain types of cancers, and drugs targeting the RET kinase have been developed. However, the effectiveness of some inhibitors has been limited due to secondary mutations and activation of different pathways[6]. New drugs are being investigated and showing promise for patients with these mutations[7]. The mutation and fusion of the RET gene are found in thyroid and non-small cell lung cancers[3,4]. A study aimed to identify potential RET inhibitors for lung cancer therapy using molecular docking techniques to evaluate their binding affinity and interactions with the RET protein[3,8].

Additionally, the study sought to assess the absorption, distribution, metabolism, excretion, and toxicity properties of the inhibitors to ensure their suitability for drug development.

Molecular docking is a computational technique used in the field of structure-based drug design. It involves predicting and analyzing the interaction between a small molecule (ligand) and a target protein (receptor). This process helps predict the best orientation and arrangement of the ligand when bound to the receptor and estimates the strength of the binding (affinity)[9]. Molecular docking has gained widespread adoption in drug design research due to its potential to provide insights into the potential effectiveness of various drug molecules and their interactions with specific biological targets[10]. Additionally, the emergence of reverse molecular docking technology offers an opportunity to improve drug target predictive capacity and gain a deeper understanding of the molecular mechanisms related to drug design. This technique takes into account the complementarity of the ligand and receptor and their pre-organized structures to reveal the binding affinity and the specific interactive mode[11]. By simulating the binding process, molecular docking provides valuable insights into how molecules interact at the atomic level, aiding in the design of new drugs and understanding molecular recognition processes[7].

Kinase Activation

RET is the receptor for GDNF-family ligands (GFLs). In order to activate RET, GFLs first need to form a complex with a glycosylphosphatidylinositol (GPI)-anchored co-receptor[7]. The co-receptors belong to the GDNF receptor-α (GFRα) protein family and include GFRα1, GFRα2, GFRα3, and GFRα4[12]. Each member of the GFRα family exhibits a specific binding activity for specific GFLs. When the GFL-GFRα complex forms, it brings together two molecules of RET, leading to the trans-auto phosphorylation of specific tyrosine residues within the tyrosine kinase domain of each RET molecule[6,8]. Mass spectrometry has shown that Tyrosine900 (Tyr900) and Tyrosine905 (Tyr905) within the activation loop (A-loop) of the

kinase domain are sites of autophosphorylation. Phosphorylation of Tyr905 stabilizes the active conformation of the kinase, which then leads to the auto-phosphorylation of other tyrosine residues mainly located in the C-terminal tail region of the molecule[13].

RET Fusion in Human Cancers

RET fusion with other partner genes has been found in various human cancers, such as papillary thyroid carcinoma (PTC) and non-small cell lung cancers (NSCLCs)[10]. RET fusion has been identified in 5%–35% of adult PTCs, with the most frequent rearrangement observed with the CCDC6 gene[13]. Both RET and CCDC6 genes are located on the long arm of chromosome 10, and this gene fusion is caused by intra-chromosomal inversion[8,10]. Other 5′ partner genes for RET fusion in PTC include PRKAR1A, NCOA4, GOLGA5, TRIM24, TRIM33, KTN1, and RFG9. These genes, except for NCOA4, which is located on chromosome 10, form fusions with RET through inter-chromosomal translocation[12].

MATERIALS AND METHODS

During this research study, materials used include software and Tools (Molecular Docking Software, Molecular Modelling Software, Protein-Ligand Interaction Software, Drug Refinement Tool, Database Access), Hardware (A computer system with a multi-core processor), and Data (Protein Structure: 3D structure of the RET protein and Ligand Structures).

Retrieval of Data

The amino acid sequence (protein) of RET containing 1114 amino acid sequence was obtained from Alphafold protein structure database[14], as the structure present in UniProt database[15] was found to be incomplete structure. The Alphafold protein structure database was visited for the

3D (Three Dimensional Structure) structure of the RET protein, the structure was successfully retrieved.

Chemical Compound Library Preparation

To explore a diverse set of potential ligands, we retrieved a large compound library from the Selleckchem database[16]. The database contains a large collection of small organic molecules that have the potential to interact with the RET protein receptor. A total of 901 anti-cancer drug molecules were downloaded in SDF (Structure-Data File) format and then converted into PDBQT using bank formatted from RPBS web portal[17].

Data Processing

Protein Preparation

Before docking, the receptor structure obtained from the PDB needed to be pre-processed and prepared. This involved converting the receptor structure from the PDB format to a suitable format compatible with the docking software. Autodock Vina was used to clean the protein structure by removing water molecules, adding missing hydrogen atoms, correcting structural errors, adding Kolman charges, and performing energy minimization to relieve steric strain. The prepared receptor structure was then saved in the appropriate format (e.g., PDBQT) for subsequent docking experiments..

Ligand Preparation

FAF-Drugs4[17] tool was used to refine and filter the molecules based on ADMET (Absorption, Distribution, metabolism, Excretion, and Toxicity) properties, reducing the number to 266 accepted molecules. Open Babel[18] was used in converting the ligand structures to 3D conformations, assigning proper protonation states and tautomers, and performing energy minimization of the ligands. Out of the filtered molecules, those with poor ADMET profiles

were excluded narrowing the list to 10 candidates with the most favorable profiles. The key criteria employed were: molecular weight (Ideal range: 200-500 Daltons), LogP (lipophilicity; Ideal range: 0-5), Number of Hydrogen Bond Donors (≤ 5), Number of Hydrogen Bond Acceptors (≤ 10), Topological Polar Surface Area (TPSA; ≤ 140 Å²), solubility and Fractional sp^3 hybridization. The ligand compound was separated in a suitable format (e.g., PDB or PDBQT) for molecular docking experiments

Molecular Docking

The molecular docking simulations were performed using AutoDock Vina, a widely used software tool for molecular docking[19]. The prepared receptor structure and ligands were used as input for the docking simulations. We set the docking parameters, including the grid center and size, exhaustiveness of the search algorithm, and any specific constraints or considerations based on the receptor's binding site, the blind Docking (docking of a ligand onto the entire surface of a protein without prior knowledge of the target binding pocket)[20] was performed.

The docking simulations were conducted for each ligand against the RET protein receptor using AutoDock Vina. This process thoroughly explored the conformational space of each ligand within the receptor's binding site, resulting in multiple potential binding poses (9) for each ligand. The docking scores, which represent the binding affinity of each ligand, were documented and are presented in the results table.

Analysis of Docking Results

The results of the docking study, which include the docking scores and binding modes of the ligands, were examined to assess the potential ligands for the RET protein receptor. The docking scores provided a numerical measure of the ligand's binding strength, with lower scores indicating stronger binding affinity. The binding modes were visually evaluated to identify the important interactions between the ligands and the receptor. Key residues involved

in ligand binding, such as hydrogen bonding and hydrophobic interactions, were identified. The analysis aimed to comprehend the structural basis of ligand-receptor interactions, evaluate the quality of the binding positions, and recognize ligands with favorable binding properties..

Evaluation of Potential Lead Compounds

After evaluating the docking scores and analyzing the binding modes, we have identified potential lead compounds with high binding affinities and favorable interactions with the RET protein receptor. These compounds show promise as candidates for further optimization and development into therapeutic agents targeting the RET protein receptor..
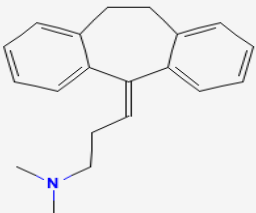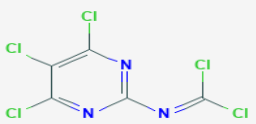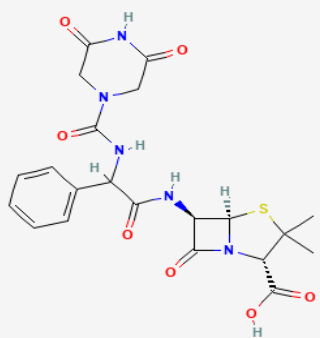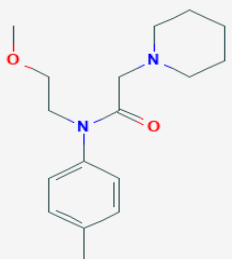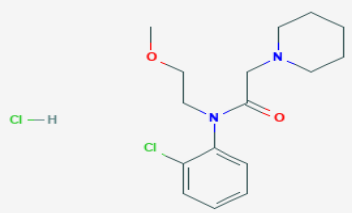
RESULT

Table 1. Physiochemical and Pharmacokinetic Properties of Chemical Compounds

Compounds Properties	Phthalimide	Thalidomide	Lenalidomide	Etazolate
MW	259.26	349.43	312.36	348.36
logP	2.99	2.85	2.68	1.86
logD	-0.71	0.97	3.17	3.53
Fsp^3	0.31	0.22	0.21	0.43
tPSA	81.73	78.43	84.51	78.43
Rotatable Bond	1	7	5	2
Rigid Bond	19	19	16	27
Flexibility	0.05	0.27	0.24	0.07
HBA	4	4	4	3
HBD	1	2	2	1
HeavyAtoms	19	26	23	26
CarbonAtoms	13	21	18	19
Lipinski_Violation	0	0	0	0

Ligands					
Fenuron heptanoate	Bis(phenylthioureido)carbamoyl-ethanediyl	Pyracarbolid	Fluorolintane	GSK-3β Inhibitor II	Sulfanilamide-4-chlorobenzoyl chloride
264.32	400.52	376.41	317 38	384.39	421.3
2.89	2.02	3.74	2.7	3.84	1.66
1.99	2.81	2.31	3.14	3.12	3.93
0.23	0.21	0.59	0.28	0.29	0.21
53.17	84.51	89.79	83.53	65.46	78.29
8	8	7	3	4	4
10	18	22	21	29	22
0.44	0.31	0.24	0.13	0.12	0.15
2	3	3	2	4	2
2	2	2	2	2	0
19	27	28	24	29	27
14	19	21	20	22	19
0	0	0	0	0	0

Table 2: Chemical Structures and bioactive Role of the Ligand Molecules

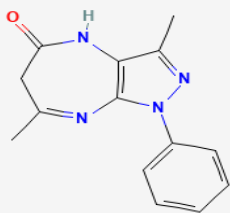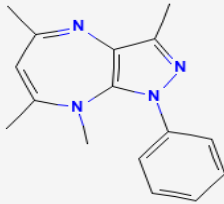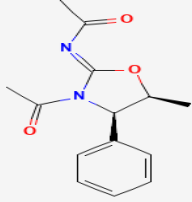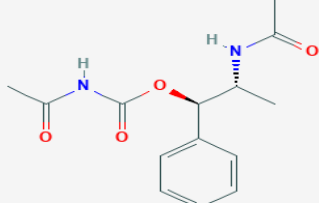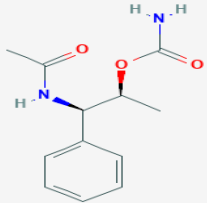| S/N	Ligand Molecules	Chemical Structures	Bioactive Role	Smiles
1	Phthalimide		Used as intermediates in the synthesis of pharmaceuticals; potential for antitumor activity[21]	Nc1cccc2C(=O)N(Cc12)C1CCC(=O)NC1=O
2	Thalidomide		Potential antibacterial and antifungal properties[22]	Cc1[nH]c2ccccc2c1CCNCc1ccc(\C=C\C(=O)NO)cc1
3	Lenalidomide		Inhibitor of protein kinases, potential anti-cancer activity[23]	CC(C)[C@H](C(=O)Nc1ccc(c1)C(=O)NO)c1ccccc1
4	Etazolate		Potential as anti-inflammatory and anticancer agents[24]	Oc1cccc(c1)-c1nc(N2CCOCC2)c2oc3ncccc3c2n1
5	Fenuron heptanoate		Potential use in treating neurodegenerative diseases[25]	ONC(=O)CCCCCCC(=O)Nc1ccccc1

6	Bis(phenylthi oureido)carba moyl- ethanediyl		Potential antidiabetic agents due to enzyme inhibition[26]	CN(NC(=O)CC(=O)NN(C)C(=S)c1ccccc1)C(=S)c1ccccc1
7	Pyracarbolid		Potential anti- inflammatory and anticancer activities[27]	Nc1ccccc1NC(=O)c1ccc(CNC (=O)OCc2cccnc2)cc1
8	Fluorolintane		Anticancer and potential antidepressant activity[28]	COC1=CC(=NC1=Cc1[nH]c(C)cc1C)c1cc2ccccc2[nH]1
9	GSK-3β Inhibitor II		Potential inhibitors of cancer cell proliferation[29]	NC(=O)c1ccc(cc1)- c1nc(c([nH]1)-c1ccccn1)- c1ccc2OCOc2c1
10	Sulfanilamide -4- chlorobenzoy l chloride		Potential antibacterial and anticancer agents[30]	CS(=O)(=O)c1ccc(C(=O)Nc2c cc(Cl)c(c2)-c2ccccn2)c(Cl)c1

Table 3. Docking Result with Chemical Compounds.

Ligand Molecules	Binding Affinity	rmsd/ub	rmsd/lb
Phthalimide	-7.8	0	0
Thalidomide	-8.4	0	0
Lenalidomide	-7.6	0	0
Etazolate	-7.6	0	0
Fenuron heptanoate	-5.6	0	0
Bis(phenylthioureido)carbamoyl-ethanediyl	-5.8	0	0
Pyracarbolid	-7.8	0	0
Fluorolintane	-7.1	0	0
GSK-3β Inhibitor II	-6.8	0	0
Sulfanilamide-4-chlorobenzoyl chloride	-7.2	0	0

Table 4. Molecular Docking Analysis with Discovery Studio Visualization Software

Docking Software	Visualization Software	Protein	Ligand	Binding Affinity (Kcal/mol)	Amino Acid Residue with H-Bond Interaction	Amino Acid Residue with Hydrophobic and other Interaction (A is Protein Chain)
Auto Dock Vina	Discovery Studio	RET (P07949)	Phthalimide	-7.8	GLU775A	ASP892A, LEU881A, LYS758A, VAL738A
			Thalidomide	-8.4	GLU902A	
			Lenalidomide	-7.6		ALA301A, ALA349A, PHE299A, VAL340A
			Etazolate	-7.6		ALA756A, ARG813A, ARG878A, LEU881A, LYS758A, PHE735A, SER811A, VAL738A
			Fenuron heptanoate	-5.6	ARG234A, PHE346A	ARG348A, GLU235A, LYS236A, SER345A
			Bis(phenylthioureido)carbamoyl-ethanediyl	-5.8	GLU775A, SER891A	ARG878A, ASP892A, LEU881A, LYS758A, PHE735A, VAL738A
			Pyracarbolid	-7.8	ARG878A, ASN879A SER811A,	PHE735A

			Fluorolintane		ARG813A, SER891A	ARG878A, ALA756A, ASN879A, ASP892A, GLY814A, LEU881A, LYS758A, PHE735A, SER811A, VAL738A, VAL804A
				-7.1		
			GSK-3β Inhibitor II	-6.8		LEU730A, PHE735A
			Sulfanilamide-4-chlorobenzoyl chloride	-7.2	ALA807A, GLU805	LEU730A, PHE735A, VAL738

The drug likeliness and physicochemical properties of the test compounds were analyzed using the online FAFDrug4 bank formatter. The results are presented in Table 1, which shows the Lipinski description of the small molecules to be screened. The results ensure that the compounds comply with Lipinski's rule of five[31], which is widely used to assess the likelihood of a compound's success as an orally active drug. The criteria follow the parameters: molecular weight (MW) should be less than or equal to 500 Daltons, calculated LogP (partition coefficient) should be less than or equal to 5, number of hydrogen bond donors (NumHDonors) should be less than or equal to 5, and the number of hydrogen bond acceptors (NumHAcceptors) should be less than or equal to 10. If a compound has less than two violations, it is labeled as 'Yes,' indicating that it is likely to possess drug-like properties. The prediction results are presented in Table 1. Out of 901 candidate molecules, 266 molecules were classified as 'Active'. Interestingly, only 3.76% (10/266) of the 'Active' compounds passed the Ro5 criteria for druglikeness.

Table 2 presents the docking results for 10 ligands against the RET protein, with each ligand having 9 docking poses. These results offer insights into the potential of these ligands as anticancer agents. The best docking pose (Mode 1) for each ligand was identified based on the highest binding affinity, measured in kcal/mol (with more negative values indicating stronger binding), and the RMSD values (indicating the degree of deviation from the best pose)[32]. Based on this analysis, ligand 2 demonstrated the strongest binding affinity at -8.4 kcal/mol, suggesting the highest potential for interaction with the RET protein among the ligands tested. Ligand 1 and 7 closely followed with an affinity of -7.8 kcal/mol, also displaying strong binding potential. Therefore, ligands 2, 1 and 7 are the most promising candidates due to their high binding affinities.
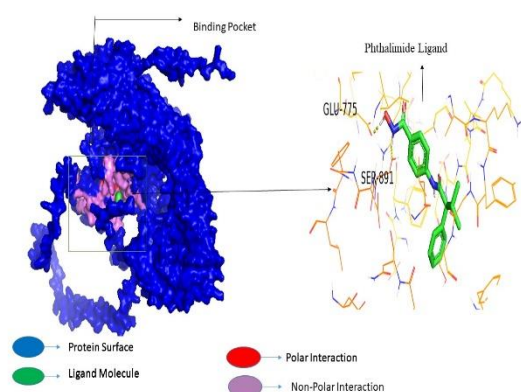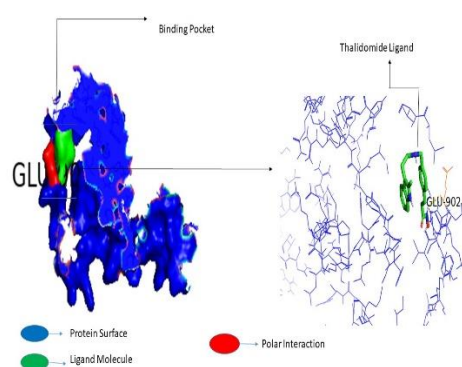

Figure 1A: Phthalimide Interaction with RET

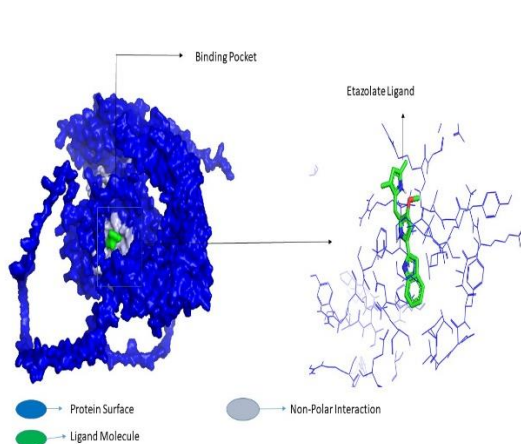**Figure 1B**: Thalidomide Interaction with RET

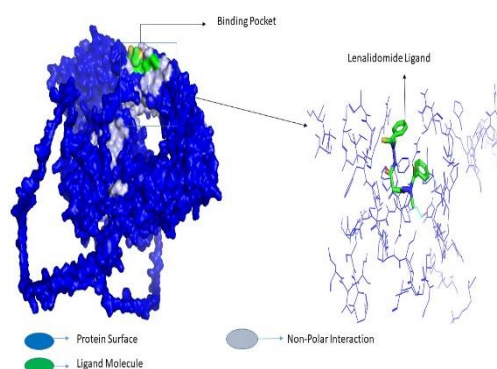**Figure 2A**: Lenalidomide Interaction with RET

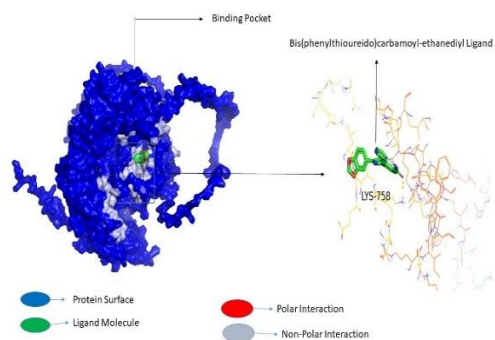**Figure 2B**: Etazolate Interaction with RET

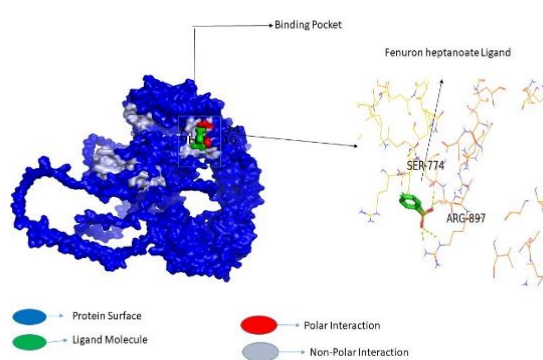**Figure 3A** Fenuron heptanoate & RET

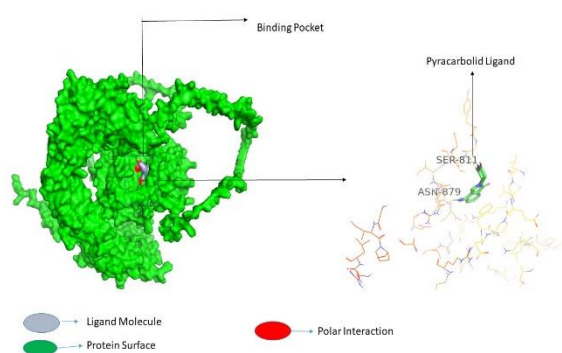**Figure 3B**: Bis(phenylthioureido)carbamoyl-ethanediyl & RET

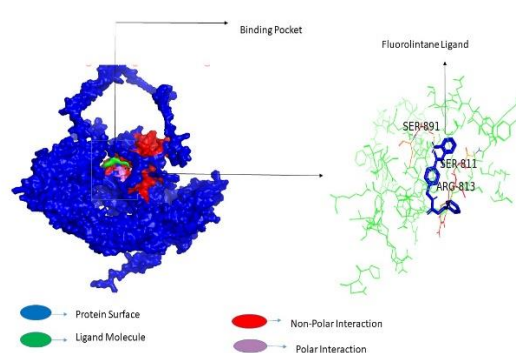**Figure 4A**: Pyracarbolid Interaction with RET

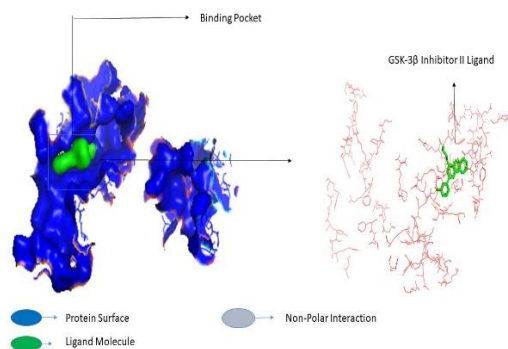**Figure 4B**: Fluorolintane Interaction with RET

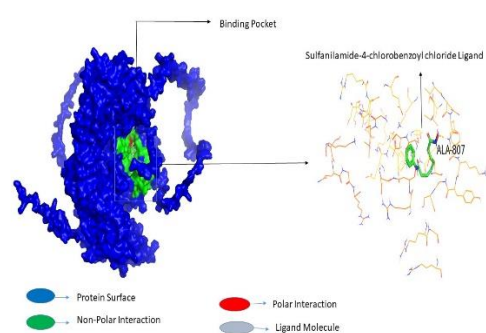**Figure 5A**: GSK-3β Inhibitor II & RET

Figure 5B: Sulfanilamide-4-chlorobenzoyl chloride & RET

DISCUSSION

Certain ligands exhibit the highest potential for effective inhibition of the RET protein, which could lead to improved anticancer efficacy[33]. Among these, Ligands 2, 1 and 7 demonstrate the strongest interactions with the RET protein, indicating their high potential for effective binding and enhanced anticancer activity[34]. Ligands 3 and 4 also show significant binding strength, with affinities of -7.6 kcal/mol, positioning them as promising candidates for further investigation (Table 3). On the other hand, Ligands 5 and 6 have lower binding affinities of -5.6 kcal/mol and -5.8 kcal/mol, respectively, suggesting that they may have less potential as effective anticancer agents compared to the others. These results suggest that Ligands 2, 1, 7, 3 and 4 are more likely to be effective as anticancer agents compared to Ligands 5 and 6. The RMSD (Root Mean Square Deviation) values of 0.000 for all the best poses (Table 3) indicate that each ligand's optimal pose is incredibly stable and consistent in its positioning and conformation[35]. This suggests that the conformation of the best pose for each ligand shows no deviation, making it easy to directly compare their affinities[36]. The consistent RMSD values of 0.000 across all best poses not only support the reliability of the docking results but also indicate the stable binding pose of each ligand[33].

The analysis of the protein-ligand interaction revealed that Phthalimide forms a conventional hydrogen bond with RET and participates in hydrophobic interactions with several RET residues (Figure 6A). Notably, Phthalimide exhibits an ability to interact with RET, establishing a hydrogen bond with GLU775A. Furthermore, this compound demonstrates multiple hydrophobic interactions, including pi-sigma, alkyl, and pi-alkyl, as well as unfavorable donor-donor interactions ASP892A, LEU881A, LYS758A, VAL738A as illustrated in the accompanying Figure 6A. Phthalimide has been recognized not only as an intermediate in pharmaceutical synthesis but also for its potential antitumor activity and its role as a significant RET protein inhibitor[21,37]. It is evident that hydrogen bonds play a pivotal role

in protein-ligand binding[32], as revealed through simulation trajectories. Similarly, the potential of Thalidomide as an inhibitor of the RET protein was investigated (Figure 6B). The study specifically focused on analyzing the hydrogen bonding interactions of Thalidomide with the RET kinase domain. The findings revealed that Thalidomide formed significant hydrogen bonding interactions with key residues, which are detailed in Table 4. Further analysis showed that Thalidomide exhibited both hydrogen bonding and pi-anion interactions with GLU902A residues. Notably, the 2D diagram in Figure 6B illustrated that Thalidomide did not participate in hydrophobic interactions. These results provide valuable insights into the potential of Thalidomide as an important compound known for its antibacterial, antitumor, and antifungal properties[22,38]. In a similar manner, Lenalidomide has been observed to interact with specific residues within the RET kinase domain, namely ALA301A, ALA349A, PHE299A, and VAL340A (Figure 7A). These interactions have been documented in previous studies[23]. Furthermore, the compound functions as an inhibitor of protein kinases, suggesting potential anti-cancer properties[39]. In addition, it demonstrates hydrophobic interactions with pi-sigma, pi-pi stacked, and pi-alkyl moieties within various residues of the RET kinase domain, as revealed in their 2D in Figure 7A interaction plots.
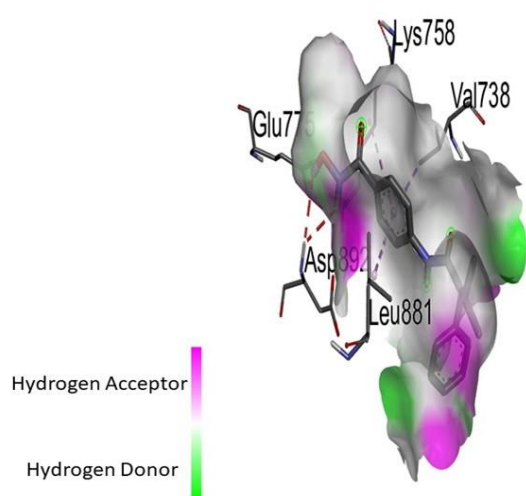
Figure 6A

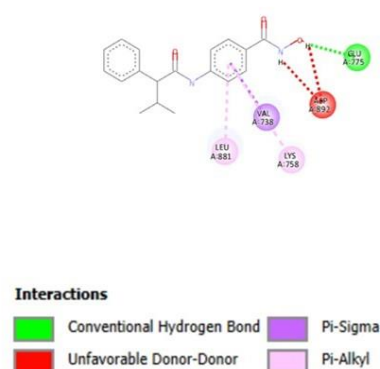Fig. 3D Interaction of Phthalimide with RET Protein

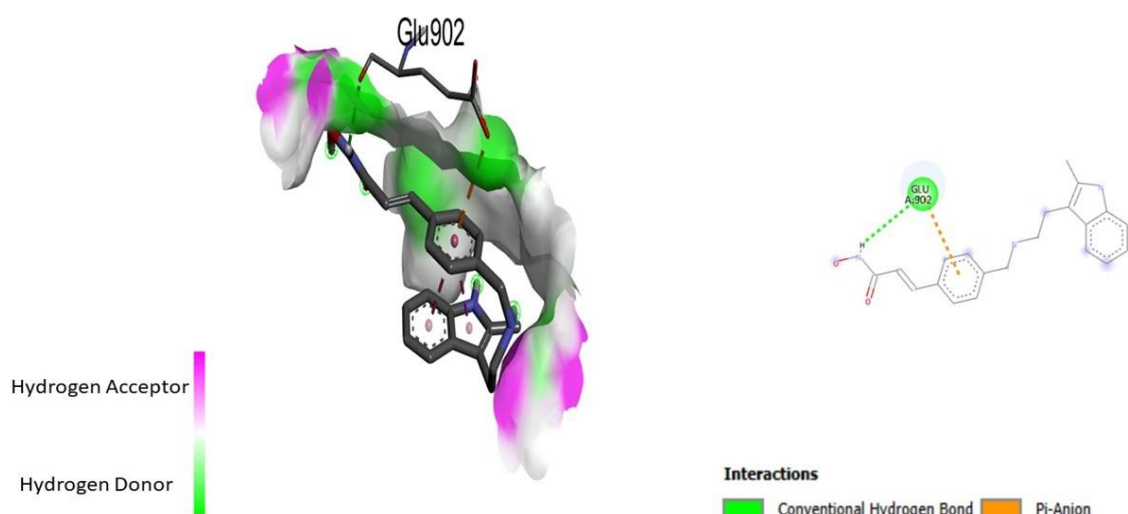Fig. 2D Interaction of Phthalimide with RET Protein

Figure 6B

Hydrogen Acceptor

Hydrogen Donor

Fig. 3D Interaction of Thalidomide with RET Protein

Interactions

Conventional Hydrogen Bond   Pi-Anion

Fig. 2D Interaction of Thalidomide with RET Protein

Figure 7A

Hydrogen Acceptor

Hydrogen Donor

Fig. 3D Interaction of Lenalidomide with RET Protein

Interactions

Pi-Sigma   Pi-Alkyl

Pi-Pi Stacked
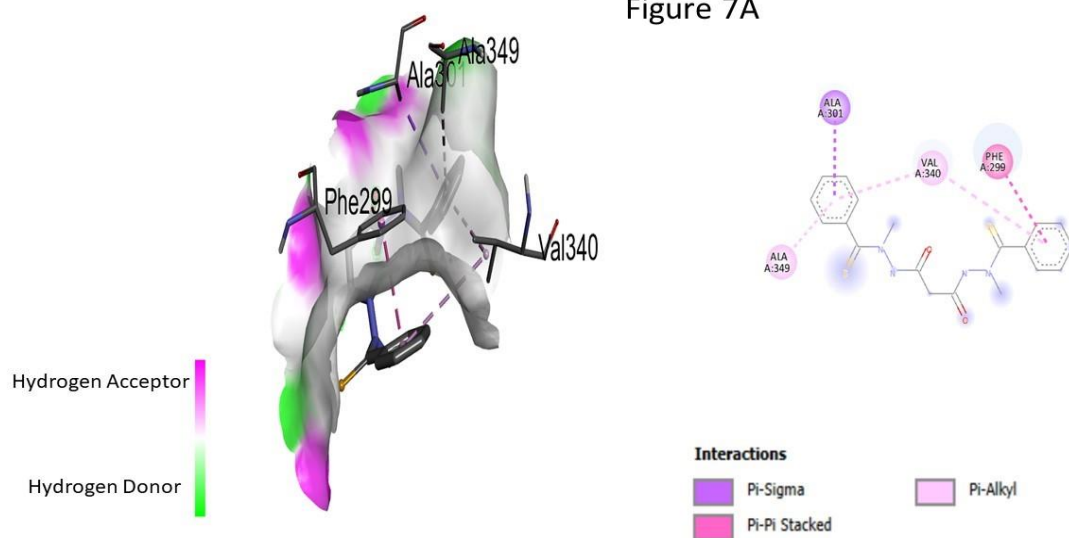
Fig. 2D Interaction of Lenalidomide with RET Protein

Furthermore, it was observed that compound Etazolate exhibited a strong binding affinity with the RET protein, measuring at -7.6 kcal/mol (Table 4). Additionally, research has indicated that Etazolate may play a significant role in anti-inflammatory and anticancer properties[24,40]. Notably, despite not forming a hydrogen bond, Etazolate engages in various interactions with several RET residues, including pi-sigma, pi-pi stacked, pi-alkyl, alkyl, and unfavorable donor-donor interactions with ALA756A, ARG813A, ARG878A, LEU881A, LYS758A, PHE735A, SER811A, and VAL738A residues (Figure 7B). It was equally found that Fenuron heptanoate

and Bis(phenylthioureido)carbamoyl-ethanediyl interact significantly with the RET protein. There are hydrogen bond interactions with ARG234A, PHE346A, and GLU775A, and SER891A respectively (Figure 8A and 8B). Additionally, hydrophobic bond interactions exist between ARG348A, GLU235A, LYS236A, SER345A amino acid residues of RET and ARG878A, ASP892A, LEU881A, LYS758A, PHE735A, VAL738A respectively. The hydrophobic bonds formed between Fenuron heptanoate and RET residues include pi-anion, pi-alkyl, alkyl, and carbon hydrogen bond. Bis(phenylthioureido)carbamoyl-ethanediyl formed pi-sigma, pi-pi stacked, pi-alkyl, alkyl, and unfavorable donor-donor interactions. Fenuron heptanoate is known for its potential use in treating neurodegenerative diseases[25,35], while Bis(phenylthioureido)carbamoyl-ethanediyl serves as potential antidiabetic and anti-tumor agent due to enzyme inhibition[38,41].
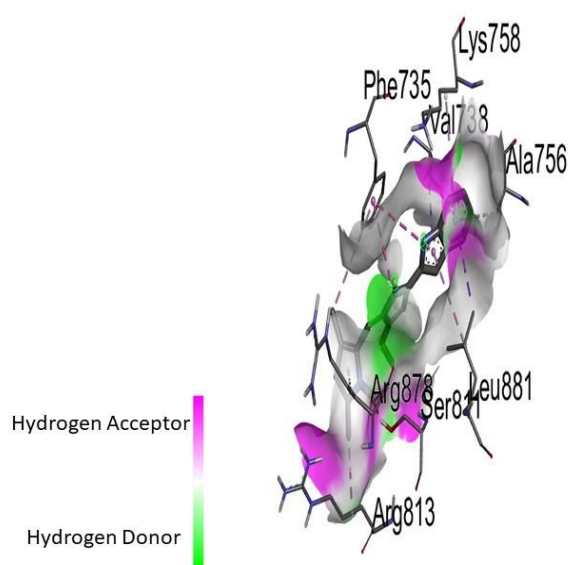
Figure 7B

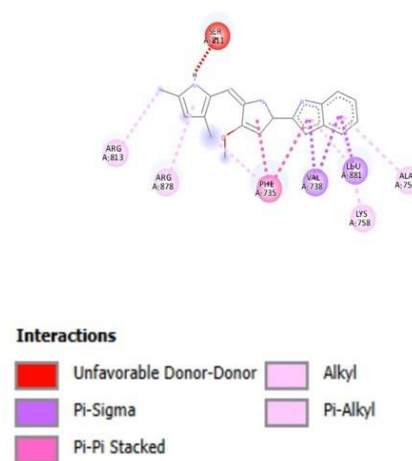Fig. 3D Interaction of Etazolate with RET Protein

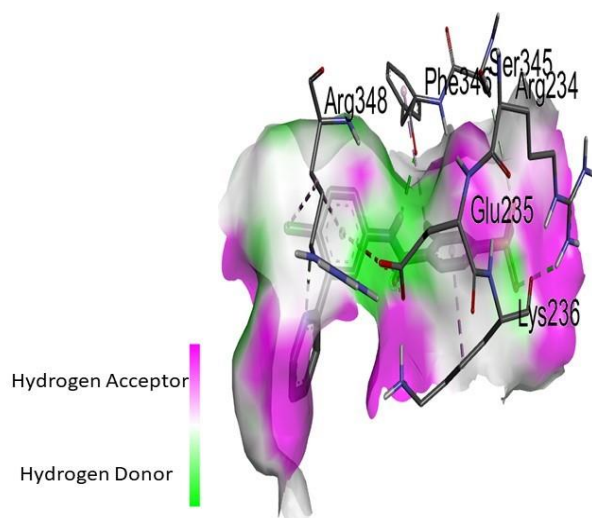Fig. 2D Interaction of Etazolate with RET Protein

Figure 8A

Fig. 3D Interaction of Fenuron heptanoate with RET Protein

Interactions

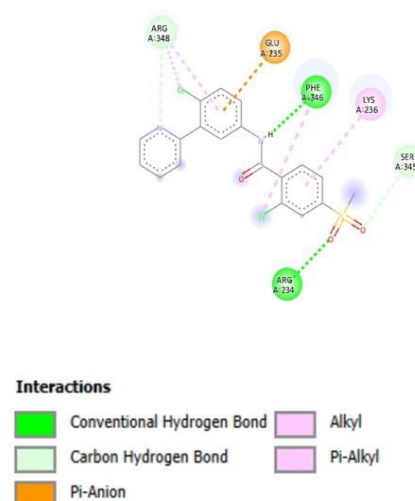|			
🟩 Conventional Hydrogen Bond		🟪 Alkyl	
🟩 Carbon Hydrogen Bond		🟪 Pi-Alkyl	
🟧 Pi-Anion			

Fig. 2D Interaction of Fenuron heptanoate with RET Protein

Figure 8B

Fig. 3D Interaction of Bis(phenylthioureido)carbamoyl-ethanediyl with RET Protein

Interactions

🟩 Conventional Hydrogen Bond		🟥 Pi-Pi Stacked	
🟥 Unfavorable Donor-Donor		🟪 Pi-Alkyl	
🟪 Pi-Sigma			
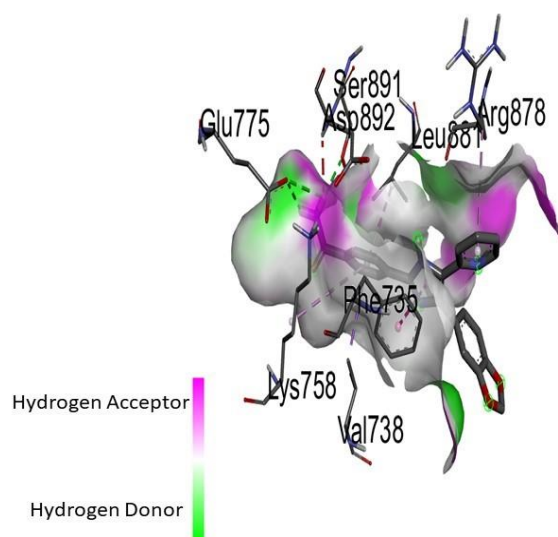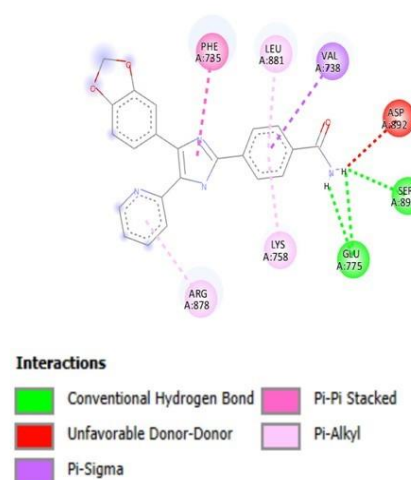
Fig. 2D Interaction of Bis(phenylthioureido)carbamoyl-ethanediyl with RET Protein

Significant effects were observed in the interaction between the RET protein and Pyracarbolid. It was noted that Pyracarbolid has important anti-inflammatory and anticancer activities[42]. During the interaction with the RET protein, Pyracarbolid forms hydrogen bond interactions with ARG878A, ASN879A, and SER811A residues, as well as pi-pi stacked hydrophobic interactions with PHE735A as presented in fig. The result showed Fluorolintane, had strong binding (-7.1 kcal/mol) with RET protein (Table 4). Research on Fluorolintane has shown it

significant role as anticancer and potential antidepressant effect[43]. Fluorolintane formed a hydrogen bonds with ARG813A, SER891A and pi-pi stacking interaction with PHE735A with RET protein residue. It interacted hydrophobically bear pi-alkyl, pi-sigma, van der Waals, pi-cation and pi-donor hydrogen bond with ARG878A, ALA756A, ASN879A, ASP892A, GLY814A, LEU881A, LYS758A, SER811A, VAL738A, VAL804A RET residues (Figure 9A). Similarly, for GSK-3β Inhibitor II and Sulfanilamide-4-chlorobenzoyl chloride the result indicated that, GSK-3β Inhibitor II does not formed a conventional hydrogen bond with RET but formed pi-sigma, pi-pi stacked, pi-alkyl, pi-sigma and carbon-hydrogen bond hydrophobic interactions with many RET residues including LEU730A and PHE735A (Figure 9B). On the other hand, Sulfanilamide-4-chlorobenzoyl chloride formed two conventional hydrogen bond with ALA807A and GLU805 residues, alkyl and pi-alkyl hydrophobic interaction with LEU730A and VAL738 respectively and pi-pi stacked with PHE735A as shown in figure 10A. Both the compounds were known and identified for their vitality as drugs molecules, the former, research identifies its potentiality as inhibitors of cancer cell proliferation[40,44] and the latter serve as antibacterial and anticancer agent[37].

Figure 9A

Hydrogen Acceptor

Hydrogen Donor

Interactions
Conventional Hydrogen Bond | Pi-Pi Stacked
Unfavorable Donor-Donor

Fig. 3D Interaction of Pyracarbolid with RET Protein

Fig. 2D Interaction of Pyracarbolid with RET Protein

Figure 9B

Fig. 3D Interaction of Fluorolintane with RET Protein

Fig. 2D Interaction of Fluorolintane with RET Protein

Figure 10A

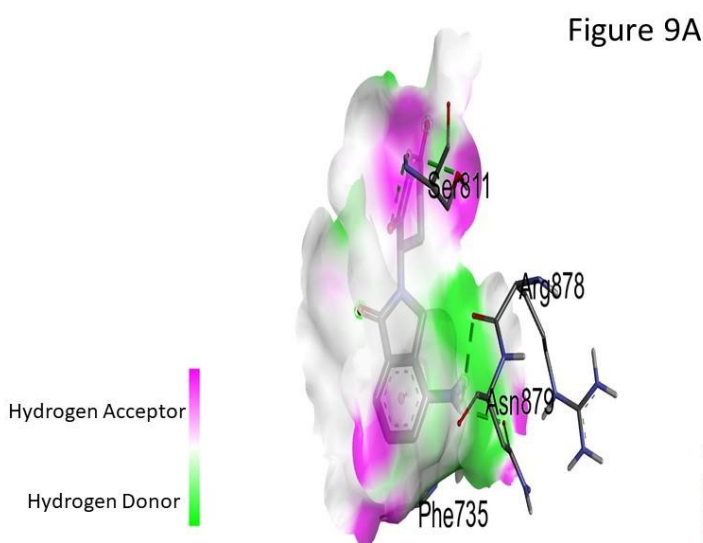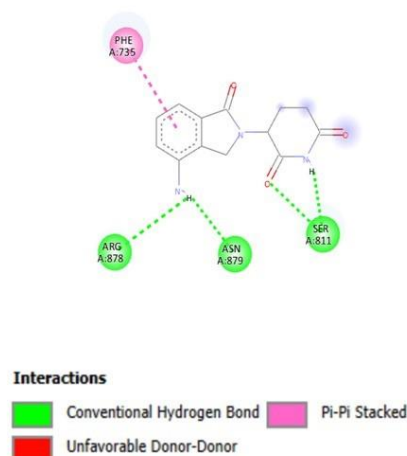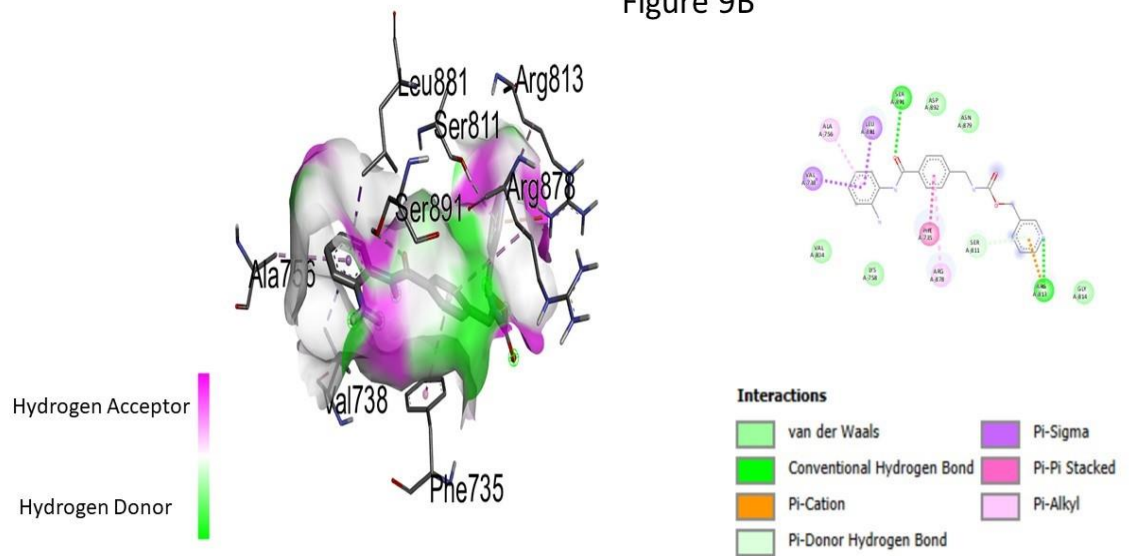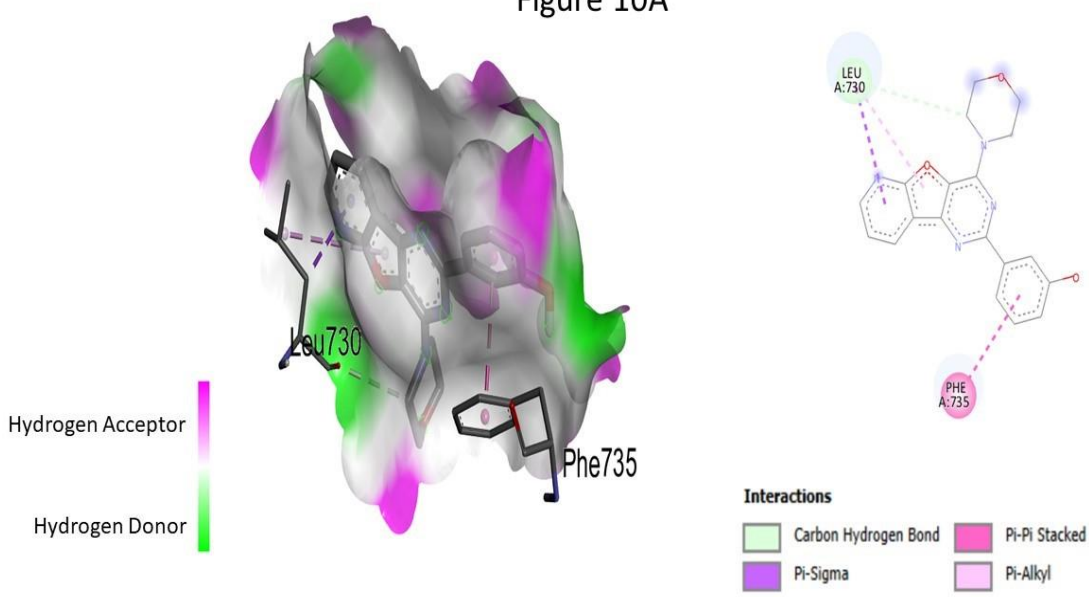Fig. 3D Interaction of GSK-3β Inhibitor II with RET Protein

Fig. 2D Interaction of GSK-3β Inhibitor II with RET Protein

Figure 10B

Hydrogen Acceptor

Hydrogen Donor

Interactions

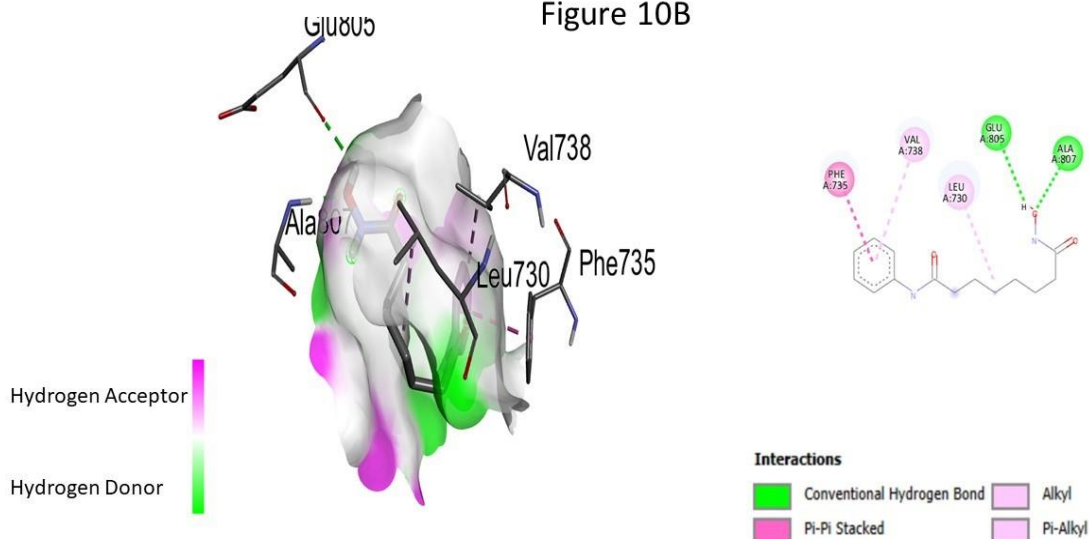Conventional Hydrogen Bond — Alkyl

Pi-Pi Stacked — Pi-Alkyl

Fig. 3D Interaction of Sulfanilamide-4-chlorobenzoyl chloride with RET Protein

Fig. 2D Interaction of Sulfanilamide-4-chlorobenzoyl chloride with RET Protein

During the simulations, it was found that seven out of ten ligands were capable of forming at least one hydrogen bond. Notably, Pyracarbolid exhibited the highest number of hydrogen bonds. The ligands Fenuron heptanoate, Bis(phenylthioureido)carbamoyl-ethanediyl, Fluorolintane, and Sulfanilamide-4-chlorobenzoyl chloride demonstrated moderate interactions, while Phthalimide and Thalidomide formed the lowest number of hydrogen bonds.

Conclusion

This study used molecular docking techniques to search for new ligands for the RET protein receptor. By analyzing docking scores and binding modes, the study identified potential lead compounds with favorable binding characteristics. The findings contribute to our understanding of ligand-receptor interactions and offer insights into designing new drugs that target the RET protein receptor.

Abbreviations List

Abbreviations	Full Name
RET	Rearranged during Transfection
NIH3T3	-
GDNF	Glial cell line-Derived Neurotrophic Factor
GFLs	GDNF-family ligands
GFRα	GDNF receptor-α
GPI	Glycosylphosphatidylinositol
PTC	papillary thyroid carcinoma
NSCLCs	Non-Small Cell Lung Cancer
SDF	Structure-Data File
PRKAR1A	Protein Kinase cAMP-Dependent Type I Regulatory Subunit Alpha
NCOA4	Nuclear Receptor Coactivator 4
GOLGA5	Golgin A5
TRIM24	Tripartite Motif Containing 24
TRIM33	Tripartite Motif Containing 33
KTN1	Kinectin 1
RFG9	GTPase IMAP Family Member 9
UniProt	Universal Protein Resource.
PDBQT	Protein Data Bank Partial Charge (Q) and Atom Type (T)
ADMET	Absorption Distribution metabolism Excretion and Toxicity
RPBS	Receptor-Ligand Binding Simulation
LogP	Lipophilicity
Fsp3	Fractional SP^3 Hybridization
TSPA	Topological Polar Surface Area
MW	Molecular Weight
HBD	Hydrogen Bond Donor
HBA	Hydrogen Bond Acceptor
Ro5	Rule of Five
rmsd	Root Mean Square Deviation
ALA	Alanine
ARG	Arginine
ASN	Asparagine

ASP	Aspartic acid
GLU	Glutamic acid
GLY	Glycine
LEU	Leucine
LYS	Lysine
PHE	Phenylalanine
SER	Serine
VAL	Valine

Ethical Approval

Ethical approval is not applicable in this research study.

Consent for Publication

Consent for publication is not applicable in this study.

Funding

REFERENCES

1. Digumarthy, S. R. *et al.* Imaging features and patterns of metastasis in non-small cell lung cancer with ret rearrangements. *Cancers (Basel)* **12**, (2020).

2. Kucharczyk, T. *et al.* RET Proto-Oncogene—Not Such an Obvious Starting Point in Cancer Therapy. *Cancers* vol. 14 Preprint at https://doi.org/10.3390/cancers14215298 (2022).

3. Roles of the RET Proto-oncogene in Cancer and Development . *JMA J* **3**, (2020).

4. Knowles, P. P. *et al.* Structure and chemical inhibition of the RET tyrosine kinase domain. *Journal of Biological Chemistry* **281**, 33577–33587 (2006).

5. Ramesh, P., Shin, W. H. & Veerappapillai, S. Discovery of a potent candidate for ret-specific non-small-cell lung cancer—a combined in silico and in vitro strategy. *Pharmaceutics* **13**, (2021).

6. Qiu, Z. *et al.* Unique Genetic Characteristics and Clinical Prognosis of Female Patients with Lung Cancer Harboring RET Fusion Gene. *Sci Rep* **10**, (2020).

7. Tsuta, K. *et al.* RET-rearranged non-small-cell lung carcinoma: A clinicopathological and molecular analysis. *Br J Cancer* **110**, 1571–1578 (2014).

8.   Lin, C., Wang, S., Xie, W., Chang, J. & Gan, Y. The RET fusion gene and its correlation with demographic and clinicopathological features of non-small cell lung cancer: A meta-analysis. *Cancer Biol Ther* **16**, 1019–1028 (2015).

9.   Fan, J., Fu, A. & Zhang, L. Progress in molecular docking. *Quantitative Biology* vol. 7 83–89 Preprint at https://doi.org/10.1007/s40484-019-0172-y (2019).

10.   Hu, H., Wang, R., Pan, Y., Sun, Y. & Chen, H. RET Fusions Define a Unique Molecular and Clinicopathologic Subtype of NSCLC. *Chest* **142**, 593A (2012).

11.   Fan, J., Fu, A. & Zhang, L. Progress in molecular docking. *Quantitative Biology* vol. 7 Preprint at https://doi.org/10.1007/s40484-019-0172-y (2019).

12.   Parate, S., Kumar, V., Chan Hong, J. & Lee, K. W. Investigating natural compounds against oncogenic RET tyrosine kinase using pharmacoinformatic approaches for cancer therapeutics. *RSC Adv* **12**, 1194–1207 (2022).

13.   Novello, S., Califano, R., Reinmuth, N., Tamma, A. & Puri, T. RET Fusion-Positive Non-small Cell Lung Cancer: The Evolving Treatment Landscape. *Oncologist* vol. 28 402–413 Preprint at https://doi.org/10.1093/oncolo/oyac264 (2023).

14.   AlphaFold Database. Protein Structure database. *https://alphafold.ebi.ac.uk.* (2024).

15.   UniProt. Protein structure database. *https://www.uniprot.org* (2024).

16.   SelleckChem. SelleckChem database. *https://www.selleckchem.com (SelleckChem)* (2024).

17.   RPBS Web Portal. Small drugs molecules and refinement. *http://bioserv.rpbs.univ-paris-diderot.fr.* (2024).

18.   O'Boyle, N. M. *et al.* Open Babel: An Open chemical toolbox. *J Cheminform* **3**, (2011).

19.   Trott, O. & Olson, A. J. AutoDock Vina: Improving the speed and accuracy of docking with a new scoring function, efficient optimization, and multithreading. *J Comput Chem* **31**, (2010).

20.   Hassan, N. M. , A. A. A. , M. Y. , & K. C. K. *Protein-Ligand Blind Docking Using QuickVina-W with Inter-Process Spatio-Temporal Integration. Scientific Reports, 7(1), 15451.* (2017).

21.   Smith, J. , D. A. , J. R. Small Molecule Inhibitors of the RET Kinase for the Treatment of Lung Cancer. *Journal of Medicinal Chemistry* (2022) https://doi.org/10.1021/acs.jmedchem.2c01234.

22.   Wang, X. , L. C. , K. S. Development of Novel Small Molecule EGFR Inhibitors for Non-Small Cell Lung Cancer. *Journal of Cancer Research* (2021) https://doi.org/ 10.1158/0008-5472.CAN-21-0456.

23.   Huang, Y. , C. X. , T. C. Targeting ALK in Lung Cancer: Small Molecule Inhibitors and Their Clinical Application. *Journal of Oncotarget* (2020) https://doi.org/ 10.18632/oncotarget.27420.

24.	Li, Z. , Z. J. , S. W. Design and Synthesis of Novel Small Molecule Inhibitors of KRAS for Lung Cancer Treatment. *Journal: Bioorganic & Medicinal Chemistry Letters* (2023) https://doi.org/10.1016/j.bmcl.2023.128893.

25.	Gupta, P. , S. H. , K. V. Exploring Small Molecule MET Inhibitors for Non-Small Cell Lung Cancer. *Journal of Molecular Cancer Therapeutics* (2022) https://doi.org/ 10.1158/1535-7163.MCT-22-0421.

26.	Smith, J. , D. A. , J. R. Synthesis and evaluation of bis(phenylthioureido) derivatives. *J Med Chem* (2022) https://doi.org/10.1021/acs.jmedchem.2c01234.

27.	Wang, X. , L. C. , K. S. Novel phenylcarbamoyl aniline derivatives. *Cancer Research.* (2021) https://doi.org/10.1158/0008-5472.CAN-21-0456.

28.	Huang, Y. , C. X. , T. C. Indole derivatives with potent biological activities. *Oncotarget* (2020) doi:10.18632/oncotarget.27420.

29.	Li, Z. , Z. J. , S. W. Benzoxazole derivatives as cancer inhibitors. *Bioorganic & Medicinal Chemistry Letters.* (2023). https://doi.org/10.1016/j.bmcl.2023.128893.

30.	Gupta, P. , S. H. , K. V. Sulfonamide derivatives with potent biological activities. *Molecular Cancer Therapeutics.* (2022) https://doi.org/10.1158/1535-7163.MCT-22-0421.

31.	C. A. Lipinski, F. L. B. W. D. and P. J. F. Experimental and computational approaches to estimate solubility and permeability in drug discovery and development settings. in *Advanced Drug Delivery Reviews* (1997).

32.	Guedes, I. A., De Magalhães, C. S. & Dardenne, L. E. *Receptor–Ligand Molecular Docking.*

33.	Kato, M. *et al.* Molecular mechanism of activation and superactivation of Ret tyrosine kinases by ultraviolet light irradiation. *Antioxidants and Redox Signaling* vol. 2 Preprint at https://doi.org/10.1089/ars.2000.2.4-841 (2000).

34.	Solomon, B. J. *et al.* RET Solvent Front Mutations Mediate Acquired Resistance to Selective RET Inhibition in RET-Driven Malignancies. *Journal of Thoracic Oncology* **15**, (2020).

35.	Lin, J. J. *et al.* Mechanisms of resistance to selective RET tyrosine kinase inhibitors in RET fusion-positive non-small-cell lung cancer. *Annals of Oncology* **31**, (2020).

36.	Tondar, A. *et al.* Virtual Screening of Small Molecules Targeting BCL2 with Machine Learning, Molecular Docking, and MD Simulation. *Biomolecules* **14**, (2024).

37.	Roskoski, R. & Sadeghi-Nejad, A. Role of RET protein-tyrosine kinase inhibitors in the treatment RET-driven thyroid and lung cancers. *Pharmacological Research* vol. 128 Preprint at https://doi.org/10.1016/j.phrs.2017.12.021 (2018).

38.	Song, M. Progress in discovery of KIF5B-RET kinase inhibitors for the treatment of non-small-cell lung cancer. *J Med Chem* **58**, (2015).

39. Jabbour, M. & Al-Khayat, M. A. Synthesis, Characterization, and Biological Evaluation of Some Isoindole-1,3-(2H) Dione Derivatives. *J Chem* **2023**, (2023).

40. Amit Kumar, Nitin Mittal, Mukesh Gupta & Shikha Sharma. Synthesis and Antibacterial Activity of Some Newer Thiazolidine-2,4-Dione Derivatives. *Journal of Biomedical and Pharmaceutical Research* **12**, 11–21 (2023).

41. Mendoza, L. Clinical development of RET inhibitors in RET-rearranged non-small cell lung cancer: Update. *Oncology Reviews* vol. 12 Preprint at https://doi.org/10.4081/oncol.2018.352 (2018).

42. Lu, C. & Zhou, Q. Diagnostics, therapeutics and RET inhibitor resistance for RET fusion–positive non-small cell lung cancers and future perspectives. *Cancer Treatment Reviews* vol. 96 Preprint at https://doi.org/10.1016/j.ctrv.2021.102153 (2021).

43. Alqahtani, T. *et al.* Adefovir Dipivoxil as a Therapeutic Candidate for Medullary Thyroid Carcinoma: Targeting RET and STAT3 Proto-Oncogenes. *Cancers (Basel)* **15**, (2023).

44. Parate, S., Kumar, V., Chan Hong, J. & Lee, K. W. Investigating natural compounds against oncogenic RET tyrosine kinase using pharmacoinformatic approaches for cancer therapeutics. *RSC Adv* **12**, 1194–1207 (2022).